frontiers | Frontiers in Earth Science

TYPE Original Research
PUBLISHED 22 February 2023
DOI 10.3389/feart.2023.1001489

OPEN ACCESS

EDITED BY
Jianwei Feng,
China University of Petroleum, China

REVIEWED BY
Vincenzo Tripodi,
Research Institute for Hydrogeological Protection (CNR), Italy
Hao Yu,
Southwest Petroleum University, China
Kaizong Xia,
Institute of Rock and Soil Mechanics (CAS), China

*CORRESPONDENCE
Kai Zhang,
reservoirs@163.com

SPECIALTY SECTION
This article was submitted to Structural Geology and Tectonics, a section of the journal Frontiers in Earth Science

RECEIVED 23 July 2022
ACCEPTED 01 February 2023
PUBLISHED 22 February 2023

CITATION
Wang Z, Zhang K, Wu Q, Zhou H, Yu S and Li Y (2023), Structural evolution characteristics and genesis of buried hill faults in the Chengdao–Zhuanghai area. *Front. Earth Sci.* 11:1001489. doi: 10.3389/feart.2023.1001489

Structural evolution characteristics and genesis of buried hill faults in the Chengdao–Zhuanghai area

Zhiwei Wang[1,2], Kai Zhang[1]*, Qunhu Wu[2], Hongke Zhou[2], Shina Yu[2] and Yang Li[2]

[1]School of Petroleum Engineering, China University of Petroleum, Qingdao, China, [2]Haiyang Oil Production Plant, Shengli Oilfield Company, Sinopec, Dongying, China

The buried hills in the Chengdao–Zhuanghai area are rich in oil and gas resources, and their structures exhibit complex styles with unique evolutionary characteristics. Based on the most recent exploration progress in this region, the structural characteristics and active parameters of the buried hill faults in this region were quantitatively analyzed using the balanced section technique. In addition, the structural evolution process of the study area was reproduced by combining the structural-physical simulation experiment. Its spatio-temporal evolution characteristics and genesis mechanisms were also systematically investigated. As observed, the study area developed three basic sets of fault systems: the NW-trending extensional strike-slip fault, the NNE-trending left-handed compression–torsion fault, and the near-EW-trending extensional fault. The study area was further segmented into six buried hills: West Row Hill, Middle Row Hill, East Row Hill, Zhuanghai Buried Hill, Zhuangxi Buried Hill, and Changdi Buried Hill. The inner fault of the NW-trending Buried Hill is a strike-slip extensional fault that formed under the influence of the right-lateral strike-slip activity of the NW-trending Chengbei Fault from the Late Jurassic to the Early Cretaceous. In particular, the NNE-trending fault was a left-handed compression–torsion fault that formed under the left-handed strike-slip activity and regional compression stress field of the Tanlu fault zone. The near-EW fault was closely related to the near-SN extension stress field in the Late Cretaceous. Since the late Triassic, the study area has experienced six evolution stages, namely, overall uplift erosion (T_3), overall coating deposition (J_{1+2}), fault segmentation (J_3-K_1), extrusion uplift differentiation (K_2), middle buried hill differentiation E), and overall stable subsidence (N-Q). Its tectonic evolution was primarily controlled by the significant variations in the tectonic stress field in the study area as well as its adjacent areas since the late Triassic, which were controlled by the tectonic stress field.

KEYWORDS

buried hill, fault structure, the balanced section, evolution characteristics, Chengdao-Zhuanghai area

1 Introduction

In recent years, deep-buried hill reservoirs have served as the major field of oil and gas exploration in China, with the Chengdao–Zhuanghai area a key region for these activities in the Jiyang Depression. Affected by the superposition of the Indosinian, Yanshan, Himalayan, and other multistage tectonic movements and the strike-slip activities of the Tanlu fault zone, the buried hill features differ in diverse structural styles, and the trend of hydrocarbon accumulation in these buried hills is complex and variable. Thus far, several scholars have studied the fault system of the typical complex oil and gas accumulation area in the Bohai Sea. They have reported that the NW and NE faults in the area exhibit strike-slip characteristics and conjugate shear characteristics (Xie, 2011; Xie et al., 2021). In particular, two sets of deep and shallow fault systems developed in the Bodong Low Uplift–Bodong Sag, wherein the shallow layer mainly resided in the EW direction and displayed an *en-échelon* arrangement. In addition, typical NE- and NW-trending faults formed in the Chengdao Low Uplift. The traditional perspective states that the two groups of faults were synchronous faults (Li et al., 2014; Shi, 2021; Xin et al., 2021), but this was not completely consistent with the actual drilling results; moreover, corresponding empirical research is still lacking in this respect. Thus, typically buried hill reservoirs developed in the Chengdao–Zhuanghai area, and their formation process, enrichment regularity, and major controlling factors are all closely associated with the development of the fault system.

Considering the Mesozoic and Paleozoic fault structures in the Chengdao–Zhuanghai area as the research object and using the latest exploration data in the study area based on balanced section technology, this study quantitatively analyzes the fault structure characteristics and active parameters in the Chengdao–Zhuanghai area. Combined with the structural physical simulation experiment, we restored the key structural evolution process in the study area and clarified its control on the development of the buried hills. Accordingly, we further explored the mechanisms of regional dynamics. The two methods corroborated each other, and the spatiotemporal characteristics and genesis of the buried hill faults in the Chengdao–Zhuanghai area have been systematically studied to obtain a series of new concepts. This study aims to add to the theory of Mesozoic basin formation in the Bohai Bay Basin and provide references for deep oil and gas exploration and future development.

2 Regional geological background

The Chengdao–Zhuanghai area, located in the southeast of the Jiyang Depression, is a secondary structural unit of the Bohai Bay oil and gas basin. It is separated from the Ludong Uplift by the middle section of the Tanlu Fault to the east and is adjacent to the Huanghua Sag and Bozhong Sag by the Chengning Uplift to the west and Boonan Uplift to the north, and the Luxi Uplift by the Qiguang Fault to the south and Linqing Sag to the southwest. The study region is located at the intersection of the Bozhong Sag, Jiyang Depression, and Chengning Uplift—with a northwest trend that includes two secondary tectonic units, the Chengbei Low Uplift (southeast) and Bonan Low Uplift (west). In particular, three typically inherited boundary basement faults developed in this area, namely, the NW-trending Chengbei Fault, the NE-trending Chengbei 30 West Fault, and the NEE-trending Chengbei 30 South Fault (Figure 1).

From bottom to top, the study area includes the Archaeozoic Taishan Group (Art), Cambrian (Є), Ordovician (O), Carboniferous (C), Permian (P), Middle-Lower Jurassic (J_{1+2}), Upper Jurassic–Lower Cretaceous (J_3+K_1). Affected by the multistage tectonic movement, the remaining Mesozoic and Paleozoic strata in the study area are non-uniformly distributed. The top surface of the Paleozoic is covered by Lower-Middle Jurassic. The local area of the No. 5 Pile Fault and the southern region of the middle row hill in Chengdao have been seriously eroded, resulting in a Mesozoic boundary that is directly covered by Archaeozoic strata. The northern region of the Middle Row Hill is locally higher and seriously denuded, and the Dongying Formation directly covers the Paleozoic strata. The superposition relationship of the Cenozoic boundary's bottom surface is complex, influenced by varying strata denudation in the late Cretaceous and varying fault activity in the early Cenozoic. The stratigraphic structure characteristics of the buried hills in the study area have been determined by the distribution characteristics of the Mesozoic and Paleozoic residual strata, in addition to the superposition relationship at the key strata interface.

3 Characteristics of the buried hill faults in the Chengdao–Zhuanghai area

Based on the drilling and logging data in the study area, the seismic data have been analyzed in detail through the combination of well and seismic data. As observed, six buried hills sequentially developed in the Chengdao–Zhuanghai area from north to south and west to east, including the Chengdao West-Row Hill, Chengdao Middle-Row Hill, Chengdao East-Row Hill, Zhuanghai Buried Hill, Zhuangxi Buried Hill, and Changdi Buried Hill. Simultaneously, the study reports that the fracture forms the predominant tectonic deformation pattern in the Chengdao–Zhuanghai area, in addition to multiple dominant development directions, primarily in the NW, NNE (NE), and near-EW directions (Figure 2), and that it controls a series of NW, NNE, and near-EW buried hill interior fractures. Overall, the pattern resembles a "north-sub-south convergence" network.

3.1 Plane distribution characteristics of the fracture system

Affected by regional and local stress field variations across different periods, the fracture system in the study region has been essentially controlled by extension, extrusion, and slip. Therefore, the fault systems of various layers varied significantly with complex, diverse characteristics, exhibiting a prominent multiperiod tectonic-superposition effect (Zhang M., 2006; Jiu et al., 2013). In addition, the fault system of the lower strata (Mesozoic and Paleozoic) in the study area displayed distinct multi-directionality, with faults of various directions and properties intersecting each other to form a north–south convergence network

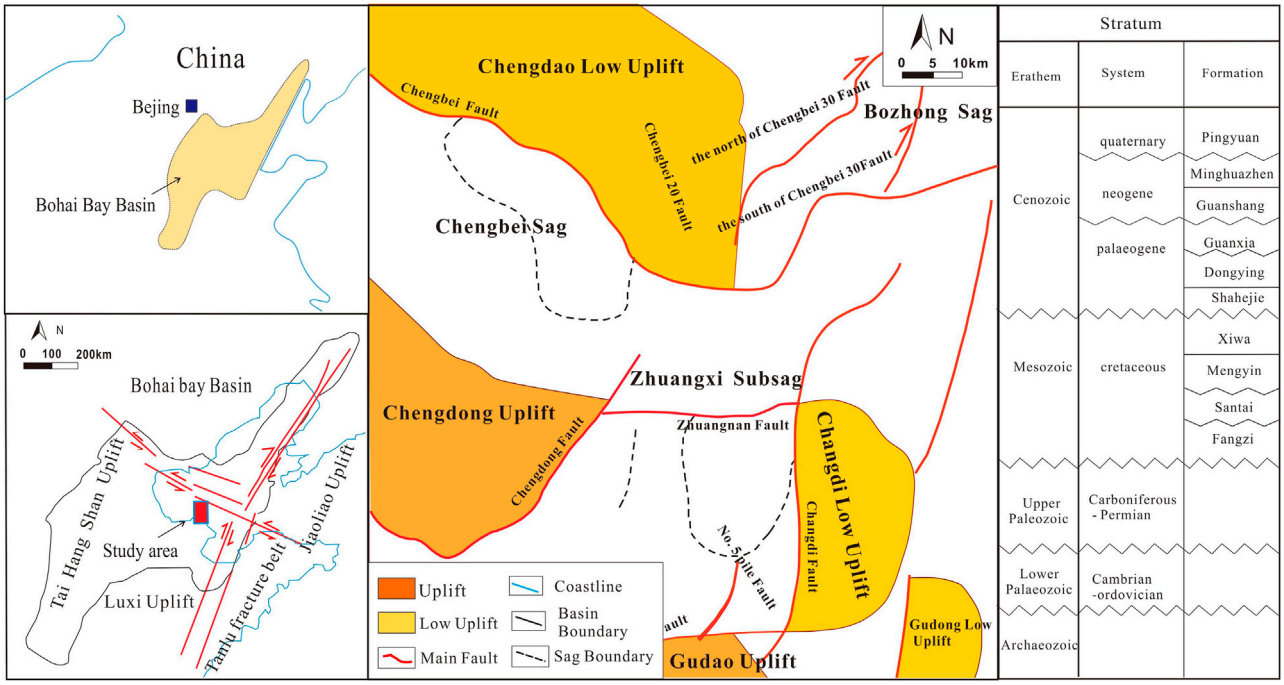

FIGURE 1
Regional tectonic background of the study area.

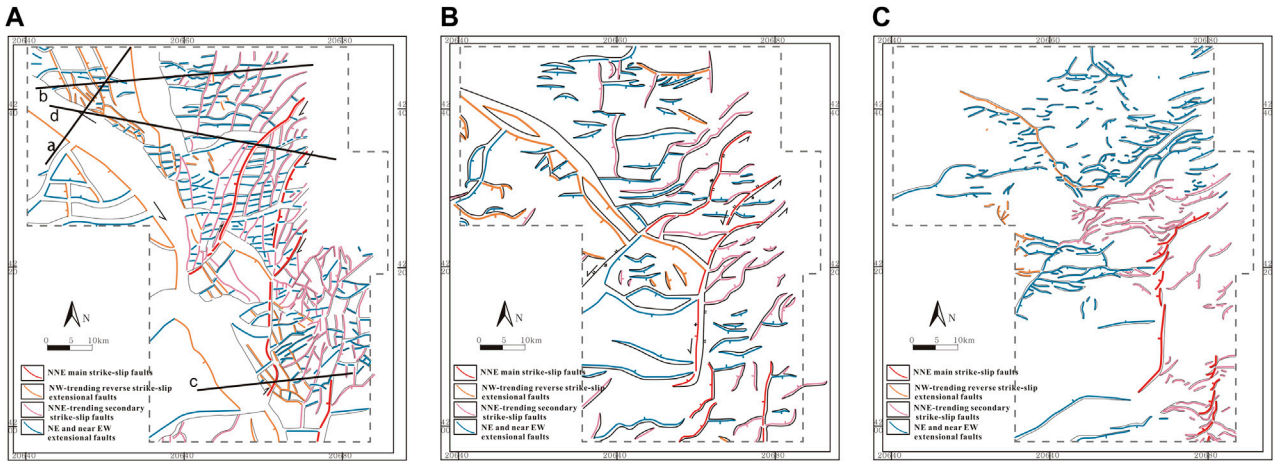

FIGURE 2
Plane distribution faults in Chengdao–Zhuanghai Area. **(A)** Plane distribution of Tg1 interface faults in Chengdao–Zhuanghai Area; **(B)** Plane distribution of Tr interface faults in Chengdao–Zhuanghai Area; **(C)** Plane distribution of T1 interface faults in Chengdao–Zhuanghai Area.

tectonic pattern. Among them, large-scale NW-trending fractures existed with numerous interior fractures, primarily along the NNE-trending and near-EW-trending directions in the area intersected by the Middle Row Hill, East Row Hill, Zhuanghai Buried Hill, and Changdi Buried Hill. In contrast, in the area of West-Row Hill and Zhuangxi Buried Hill (Figure 2A) (Zhang X., 2006; Li, 2008; Yang, 2008; Mao et al., 2019), the NW-trending and near-EW-trending inner fractures dominated. In the middle strata (Palaeogene), the NW-trending No. 5 Pile Fault and Chengbei 20 Fault gradually disappeared, and the No. 5 Pile Fault was reconstructed by the NNE-trending Changdi Fault. Although the NW-trending Chengbei Fault continued to move, the horizontal fault distance decreased significantly. All the interior faults disappeared, and numerous NNE strike-slip faults, NE-trending, and EW-trending

TABLE 1 Characteristics of the fracture system profile development in the Chengdao–Zhuanghai Area.

Type of fracture profile	Fault	Characteristics of fracture system profile
NW-trending fractures	Chengbei Fault	Chengbei Fault is the southern boundary fault of the Chengbei low uplift, which is the depression-controlling fault of the Chengbei Sag and the mountain-controlling fault of the Chengdao West Row mountain. The fault is inclined toward SW, and the shovel-shaped main section cuts deeper. The lower Paleozoic exhibits a thin bottom, and the upper portion of the fault can be combined with the secondary faults to form a "Y"-shaped, flower-like combination of the structural styles on the section
	Chengbei 20 Fault	The Chengbei 20 Fault is the mountain-controlling fault of Middle Row Hill. The fault is inclined toward SW and displays a shovel-type normal fault from north to south, with a gradually decreasing scale. The upper plate of the fault exhibited a thin bottom and was clearly thinner than the lower plate on the section
	No. 5 Pile Fault	The deep NW-trending structure of the No. 5 Pile fault was evident, whereas the shallow layer ceased the activity and gradually intersected the NNE-trending Changdi Fault from north to south. The profile is a shovel-type normal fault that does not cut through the bottom interface of the Cenozoic. The Lower Paleozoic displayed a thin or bald bottom because of the cutting and reconstruction of the Changdi fault
NNE-trending fractures	Changdi Fault	The Changdi Fault is the mountain-controlling fault of the Changdi Buried Hill, with a vertical fault plane at the section inclined toward NW, which was combined with secondary faults to form a multistage "Y"-shaped, flower-like structure in the shallow portion that cut the No. 5 Pile Fault in its deep portion. The local regions exhibited certain pressure–torsion properties, and the east side of the strata bending arch formed a forced anticline
	North and south of Chengbei 30 Faults	The north and south Chengbei 30 Faults are the mountain-controlling faults of the East Row Hill. The two faults on the section tend in opposite directions with a steep principal section. The shallow part and the secondary fault formed a flower-like, multistage "Y" combination. The north of the Chengbei 30 Fault became inactive during the Guantao Formation, whereas the south of the Chengbei 30 Fault disappeared during the Minghuazhen Formation
	Chengdong Fault	The Chengdong Fault is a major control fault in the Gubei Sag. In the profile, the North–South Fault was positive by inversion and exhibited a certain strike-slip effect. Zhuanggu 29 Fault was formed at the junction of the northernmost Chengbei Fault, and the compression–torsion effect was the strongest. In its entirety, the Chengdong Fault was characterized by normal plate- or shovel-type faults, strong shallow strike-slip action, and multilevel "Y" shape combination with secondary faults
NW-trending fractures	Chengbei 304 South Fault	The Chengbei 304 South Fault is the boundary fault between the Chengdao East Row Hill and the Zhuanghai Buried Hill. The deep layer was clear and continuous, and the shallow layer was composed of multiple parallel faults inclined toward the south with a shovel-type principal section. The upper and multiple secondary faults formed a multilevel "Y"-shaped combination with certain strike-slip properties
	South of Zhuanghai 104 Fault	The Zhuanghai 104 Fault is the controlling fault of the Zhuanghai Buried Hill, which is inclined southward with a shovel-type principal section and poses a strong control effect on the Palaeogene. The pre-Palaeogene system was cut and reformed. The upper and secondary faults merged to form the "Y"-shaped, flower-like combination with other structural styles
	Zhuangnan Fault	The Zhuangnan Fault is the mountain-controlling fault of the Zhuangxi Buried Hill, inclined southward with a shovel-type principal section. The upper and secondary faults were combined into a multilevel "Y"-shaped combination

extensional faults developed, with secondary faults increasing in the EW and NE-trending (Figure 2B) (Ma, 2018).

Due to the dominant effect of the strike-slip features, the overall number of fractures increased significantly in the upper strata (Neogene), and the primary fractures were discontinuous in all directions. More specifically, the NNE-trending fractures were composed of NEE-trending faults along the NNE-trending lateral rows, and the number of secondary faults in the west decreased, with the strike-slip effect becoming weaker (Figure 2C) (Wang et al., 2004).

3.2 Profile development characteristics of the fracture system

In the dominant fault systems of the study area, the NW trending faults are typically represented by the Chengbei Fault, Chengbei 20 Fault, and No. 5 Pile Fault; the NNE (NE) trending faults are represented by the Chengbei 30 North Fault, Chengbei 30 South Fault, Changdi Fault, and Chengdong Fault; and the near EW trending faults are represented by the Chengbei 304 South Fault, Zhuanghai 104 South Fault, and Zhuangnan Fault. Combined with extensive geophysical data, we studied the development characteristics of the fault system in detail (Table 1; Figure 3).

3.3 Control effects of the main fault system on the buried hill

The main fault system in the study area is crucial for controlling the development and evolution of the buried hills. Among them, the C–P and Є–O strata in the upper wall of the NW-trending Chengbei Fault, Chengbei 20 Fault, and No. 5 Pile Fault displayed a prominent "bare bottom" or "thin bottom", indicating that they underwent

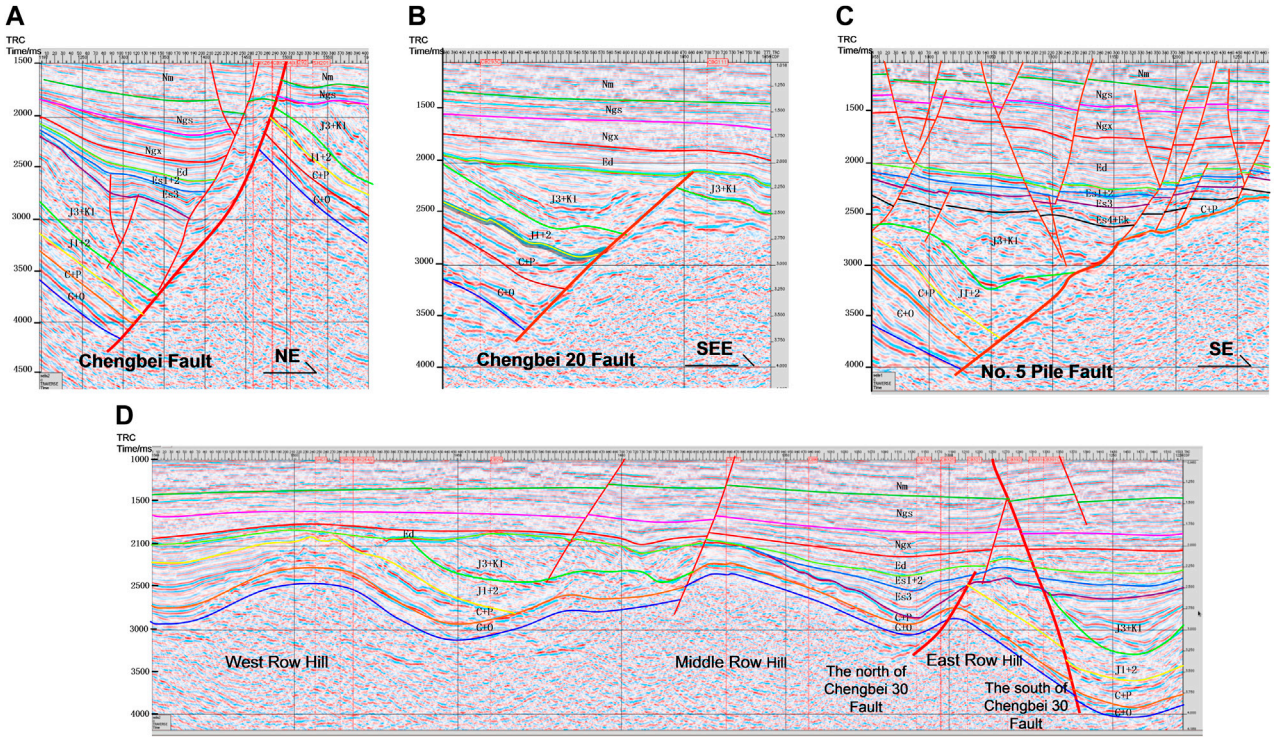

FIGURE 3
Control effect of major fault systems on buried hills. **(A)** Control effect of Chengbei Fault on buried hills; **(B)** Control effect of Chengbei 20 Fault on buried hills; **(C)** Control effect of No.5 Pile Fault on buried hills; **(D)** Control effect of Chengbei 30 Fault systems on buried hills and the distribution of buried hills.

compressional thrust in the late Triassic, resulting in strong erosion in the upper Paleozoic. During the late Jurassic to early Cretaceous, the fault occurrence caused a structural inversion from "reverse fault" to "normal fault" (Figures 3A–C), thereby shaping the NW-trending buried hill system in the area.

During this time, the NNE (NE)-trending fault started to experience sinistral tension and torsion from J_3 to K_1, and subsequently experienced compression and right-lateral tension and torsion, such that the NW-trending buried hill system was segmented into three sections: the north section and the south section, primarily controlled by the NW-trending fault and the middle section, predominantly controlled by the NNE-trending fault. Influenced by the conversion effect of the pre-existing NW-oriented Chengbei-Pile 5 fault, the combination of the NNE-oriented Chengbei 30 north and south fractures formed the NNE-trending Chengdong and NNE-trending Changdi faults, which created a graben that segmented the mountain system in the study area into the north, middle, and south sections. In addition, under the influence of the right-lateral strike-slip of the Palaeogene Tanlu Fault, the nearly north–south tectonic stress field was derived in the study area, which controlled the tensile activity of the nearly EW-trending fault and formed shovel-type normal faults such as the Zhuangnan Fault, Zhuanghai 104 South Fault, and Chengbei 304 South Fault. These faults segmented the middle portion of the NNE-trending extension buried hill formed by the Mesozoic cutting into the buried hill bodies such as the East Row Hill, Zhuanghai Buried Hill, and Zhuangxi Buried Hill (Hu, 1997; Dai and Meng, 2000; Chen and Zhang, 2002; Hou et al., 2005; Li et al., 2010).

4 Structural evolution characteristics of the buried hill faults in the Chengdao–Zhuanghai area

4.1 Analysis of fault activity of the buried hill in the Chengdao–Zhuanghai area

The activity characteristics of the faults can reflect the expansion and compression of the study area. The balanced section technique is a vital tool for studying fault activity characteristics, and its basic principle is that the stratigraphic length is always retained during deformation (Guo et al., 2012; Wei et al., 2018). The geological section of the tectonic evolution stage can be restored by layer-by-layer stripping to clarify the fault activity and evolution characteristics in each period. Under the constraint of multiple wells such as Chengbei 30 and Chengbei 304, the horizon was initially tracked using the time-domain data of the seismic profile. The tracked seismic horizon primarily included Nm, Ngs, Ngx, Es1+2, Es3, Ed, Es, J3+K1, J1+2, C+P, and Є+O, among others. The second phase involves the interpretation of the fault and the depiction of the geometry of the buried hill. The third stage involves the conversion of the time-domain data into depth-domain data, to then study the evolution of the balanced profile.

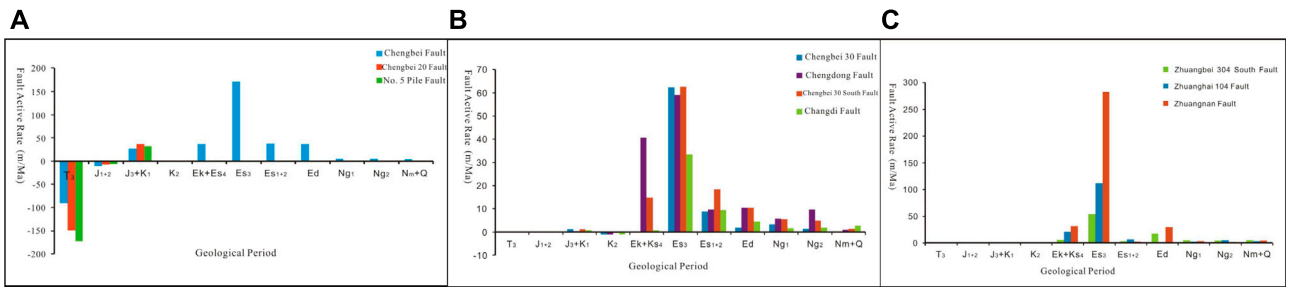

FIGURE 4
Column diagram of the fracture activity rate in the study area. **(A)** Extension rate of the NW direction survey line; **(B)** Extension rate of the NNE direction survey line; **(C)** Extension rate of the EW direction survey line.

Typical survey lines in the study area were intercepted, and the structural equilibrium evolution profiles were obtained using the equilibrium profile technique after seismic layer tracking, fault interpretation, and time-depth conversion. In the study area, the NE–SW, NWW–SEE, and near-SN sections were back-stripped on a layer-by-layer basis, and the amount of extension in each period was calculated and plotted as a histogram (Figure 4). These fault growth indices were used to characterize the influence of faults on the thickness distribution of the residual strata, in addition to the control of faults on the development of depressions and lake basins. The results revealed that the formation of the NW faults initiated in the late Triassic and displayed strongly active reverse-faulting properties, with "thin bottom" or "bald bottom" phenomena in the upper Paleozoic. Compared with the Late Triassic, the faults continued to thrust, but the intensity was low, and the activity rate was significantly reduced in the early-middle Jurassic. In the late Jurassic to early Cretaceous, the faults were tectonically reversed—from negative inversion of reverse fault to extensional normal fault—whereas in the Late Cretaceous, the faults were almost inactive, and only the Chengbei Fault remained continuously active in the Cenozoic. The intensity of the fault activity progressed from strong to weak to relatively strong to strong from Es_3–Es_2–Es_1–E_d–Ng–Nm. In contrast, the activity of the Chengbei 20 Fault and No. 5 Pile Fault ceased after entering the Cenozoic (Figure 4A). As depicted in Figure 4A, during the Triassic Period thrust, the Chengbei Fault, Chengbei 20 Fault, and No. 5 Pile Fault created an uplift and denudation of the upper and lower Palaeozoic strata in the three regions, including the thinning or loss of the strata. Between the Jurassic and the Shasi periods, these three faults exhibited less activity and gradually transformed into normal faults. Overall, the strongest fault activity occurred during the Shahejie Formation, which was the boundary fault of Chengbei Sag, Chengbei 20 West Sag, and Gubei Sag. This controlled the formation of the faulted lake basin and deposited a thick layer of shale that acted as the area's primary source of rock. The activity rate of the fault decreased as it moved from the Es2 to the Pingyuan Formation.

Compared with the NW-trending faults, the NNE-trending faults became active at a later time and started to move in the late Jurassic to early Cretaceous with weaker activity. In the late Cretaceous, they underwent EW compression and exhibited specific compression–torsion properties. In the Cenozoic (E_k–Es_4), except for the north Chengbei 30 Fault, which was inactive, the remaining faults were reactivated and started to control deposition. During Es_3, each fault was strongly active, including the north of Chengbei 30, which peaked with an activity rate of up to 65 m/Ma. Thereafter, it gradually decreased and tended to extinguish (Figure 4B). The EW-trending key fault was formed during the latest stage and started to be active in the Cenozoic, cutting and reforming the pre-Palaeogene, in the Kongdian Formation–Sha4 layer had minimal activity, and the activity rate attained its peak in the Sha3 layer—150 m/Ma.. The Kongdian Formation–Sha4 layer had minimal activity, and the activity rate attained its peak in the Sha3 layer—150 m/Ma. Following that, it tended to decline, only slightly picked up during the Ed period, and gradually weakened and stopped (Figure 4C). As can be seen in Figures 4B,C, the NNE and EW trending faults were primarily active during the Shahejie Formation period. Additionally, the high fault-activity rate under tension controlled the formation of the faulted lake basin. For instance, the Zhuanghai 104 South Fault controlled the formation of the Zhuangxi Depression.

4.2 Structural evolution characteristics of the buried hill faults in the Chengdao–Zhuanghai area

To further clarify the tectonic evolution characteristics of the buried hill faults in the Chengdao–Zhuanghai area, three lines were selected to restore the balanced section (Figures 5A–C). In accordance with the conservation principle for the section area and layer length, the balanced section was restored using the back-stripping method. The influence of denudation and deformation were considered in the process of restoring the balanced profile. The principle of constant thickness was applied to the denudation on a layer-by-layer basis in regions experiencing no structural inversion and compression deformation. The curved strata were leveled in the areas where compression formed folds. For the denuded areas, the thickness was restored by referring to the non-denuded areas. Based on the geometric relationship, 2d MOVE software was used to conduct a time-depth conversion of the seismic interpretation profile, conduct structural restoration processing for various structural components, repeat experiments, and obtain a reasonable structural evolution profile. The extension rate of each

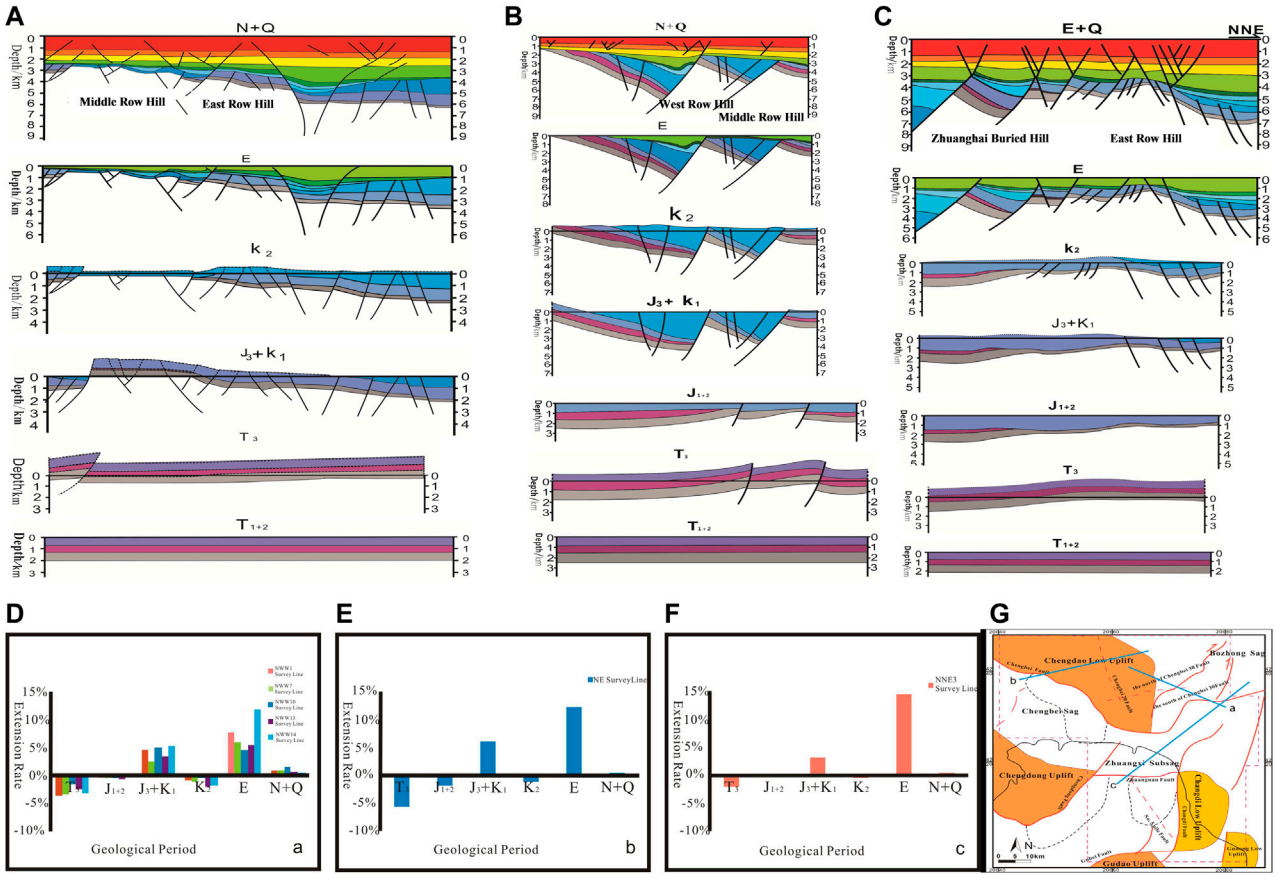

FIGURE 5
Restoration of equilibrium profile and comparison of stretching rate along various directions of the study area **(A)** Section map of the NWW direction survey line; **(B)** Section map of NE direction survey line; **(C)** Section map of the NNE direction survey line; **(D)** Extension rate of the NWW direction survey line; **(E)** Extension rate of the NE direction survey line; **(F)** Extension rate of the NNE direction survey line; **(G)** Section location.

survey line was calculated accordingly. Combined with the comprehensive analysis of the geometric characteristics, the kinematic characteristics and tectonic evolution history profile were obtained with a new understanding of the buried hill structure in the study area.

The results of the balance section demonstrated that the Chengdao–Zhuanghai area was experienced multiple stages of uplift and erosion, the extrusion and extension displayed evident stages (Figures 5D–G). In the late Triassic, the study area was controlled by a NE-trending compressive stress field, which formed a series of NW-trending thrust faults, with the evident shortening of the NE-trending survey lines. In the Early-Middle Jurassic, the study area experienced weak extrusion in the NE–SW direction, and the survey lines in all directions were somewhat shortened, with NE-trending survey lines being more pronounced in this process. In the late Jurassic to early Cretaceous, the entire study area entered the stage of fault depression, which was primarily controlled by the NE–SW-trending extensional stress field. In addition, the NW fault reversed and controlled the deposition, with a strong NE-trending line extension. By the late Cretaceous, the study area had been uplifted and eroded by a near-EW directional extrusion. By the late Cretaceous, the study area was influenced by the near-EW directional extrusion that uplifted and denuded the entire study area. More importantly, this denudation was relatively intense in the NNE directional fault compression and torsion activity area, and the NWW directional test line was significantly shortened. By the Palaeocene, the study area had entered a strong tensional fracture trap that was predominantly controlled by the near-SN-oriented extensional stress field, and the NNE-oriented measurement line exhibited a large extension rate. In the Neoproterozoic–Quaternary period, the entire research area entered a depressional stage, which slowed tectonic activity and gave each direction a low extension rate.

5 Discussion on the origin of the buried hill fault structure in the Chengdao–Zhuanghai area

5.1 Structural physics simulation experiments

To further establish the evolution process of the buried hill fault structure in the Chengdao–Zhuanghai area and explore its genetic

mechanism, we used the structural physical simulation experiment for forward modeling. The structural physical simulation experiment uses the similarity principle to reproduce the natural tectonic deformation process in a short time and on a small scale (Hu et al., 2020; Zhang et al., 2022).

The study area experienced multistage extension and compression in the Mesozoic, with strong NE–SW compression in the late Triassic–early and middle Jurassic, strong NE–SW extension in the late Jurassic–early Cretaceous, and EW compression in the late Cretaceous (Zhang et al., 2017; Jing, 2020). The faults in the studied area experienced a transformation from negative inversion to positive inversion during their development and evolution (Liu et al., 2019). The structural physical simulation experiment aims to reconstruct and restore the two stages of structural inversion experienced in the study area to provide an essential basis for the genesis of buried hill faults.

The structural physics simulation experiment was completed in two stages. During the T_3-J_3 + K_1 period, the faults in the study area experienced strong to weak compression to tensile negative inversion. In the K_2 period, the faults experienced a positive inversion of tension to compression. Here, only the two experimental groups that fit the data the best were selected for analysis.

5.1.1 Materials for the experiments

Yellow quartz sand with 80–100 mesh and blue quartz sand with 40–60 mesh sand was chosen as the experimental materials. According to the distribution of strata and lithology, the T_3–J_3+K_1 period's primary strata were the Fangzi Formation ~400 m, Santai Formation ~350 m, Mengyin and Qingshan Formation ~250 m, and its main lithology was medium and fine sandstone. In order to represent the medium and fine sandstones, 40–60 and 80–100 mesh sand were used, respectively. The early sedimentary strata were stratified with 80–100 mesh blue quartz sand, and the later sedimentary strata were stratified using 80–100 mesh bright yellow and green quartz sand. In accordance with the similarity principle, the strata thickness in the T_3–J_3+K_1 period was set at 3.5 cm, and that in the K_2 period was set at 4.5 cm. Based on the perspective of stratum thickness, T_3–J_3+K_1 was Fangzi Formation~400m, Santai Formation~350m, Mengyin and Qingshan Formation~250m thick, and K_2 was approximately 285 m thick, with a thickness ratio of 1000:285=3.5:1. Therefore, the stratum thickness in the T_3–J_3+K_1 period was set at 3.5 cm, the total stratum thickness in the K_2 period was set at 4.5 cm, and the stratum thickness in the K_2 period was 1 cm.

5.1.2 Substrate conditions and experimental model

To represent the T_3–J_3+K_1 period, rubber skin and canvas were placed at the bottom of the sandbox. After splicing these two layers, the two ends were fixed on the driving units to reflect the different properties of the substrate. During the experiment, moving the driving units to either side caused the displacement to propagate upward and deform the sand body (Figure 6A). For the K_2 period, an elastic cloth and a polystyrene simulation basin were positioned at the bottom of the sandbox. Both ends of the elastic fabric were fastened to the driving unit to achieve the transfer displacement to the upper sand body (Figure 6B).

5.1.3 Experimental process and results analysis

The tectonic physics simulation experiment for the time span T_3–J_3+K_1 lasted 63 min. At the initial stage, the left drive unit was extruded at a speed of 0.5 mm/s. At 18 min, the No. 1 Fault was generated after altering the basement properties, and the fault property corresponded to a reverse fault. The cross-section was flat, inclined on the SW, small dip angle, and continuous development. At 25 min, the left and right driving units were set to two-way tension: the tensile speed of the right drive unit was 0.4 mm/s, and the extensional displacement reached up to 0.8 mm/s. At 42 min, the extension displacement reached 2.7 cm. The smaller No. 2 and No. 3 faults were generated on the upper plate of the No. 1 Fault, both of which were positive faults inclined toward NE, during the early stage when the No. 1 Fault was structurally reversed under the influence of tensile stress, and the reverse fault was reversed from negative to positive. After conducting the simulation experiment for 49 min, fault No. 4, similar to Fault No.3, was formed in the forward direction of the No. 3 Fault. Upon running the experiment for 63 min, Fault No. 5, a positive fault that was consistent with fault No. 4, was generated in the forward direction of Fault No. 4. The upper plate of Fault No. 1 displayed a forward normal-fault layer combination (Figure 7A). The experimental results revealed that the NE–SW directional stress-field transformation in the study area initially extruded before being subjected to tension, which caused the tectonic negative reversal of the previously developed reverse faults. This finding is consistent with the general negative reversal of the NW directional faults in the T_3–J_3+K_1 period throughout the Jiyang Depression.

For the K_2 period, the duration of the tectonic physics simulation experiment was 92 min. In the initial stage of the experiment, the model was biaxially stretched. The speed of the left and right drive units was 0.08 and 0.1 mm/s, respectively. After conducting the experiment for 15 min, the No. 1 Fault - a normal fault inclined toward SE - was generated along the polystyrene foam. As the tensile displacement increased, the No. 2 Fault was produced in the upper plate of the No. 1 Fault at 32 min. A typical graben structural style was produced by the fault, which was of the normal type, inclined toward NW and forming a common descending plate with No. 1 Fault. With the continuous extension, more small-scale normal faults were generated in the fault block, including the No. 3 Fault. The fault scale continued to increase with the extension displacement. The final displacement of the tension stage was 6 cm, and the vertical fault spacing of the large boundary fault was 1 cm. After continuing the experiment for 41 min, the ensuing sedimentary strata were placed in accordance with the aforementioned experimental model. Combined with the non-uniform deformation of the previous strata, the subsequent strata were reasonably settled. The velocities of both the left and right driving units were set at −0.1 mm/s, respectively. This ensured the simultaneous extrusion of both sides of the sandbox to ensure the transformation of the stress-field properties of the model from extension to extrusion. After performing the simulation experiment for 67 min, a slight extrusion, uplift and, contraction occurred in the formation. As the extrusion displacement reached 1.9 cm, the descending plate of the first fault gradually transformed into the ascending plate, and the normal fault layer progressively

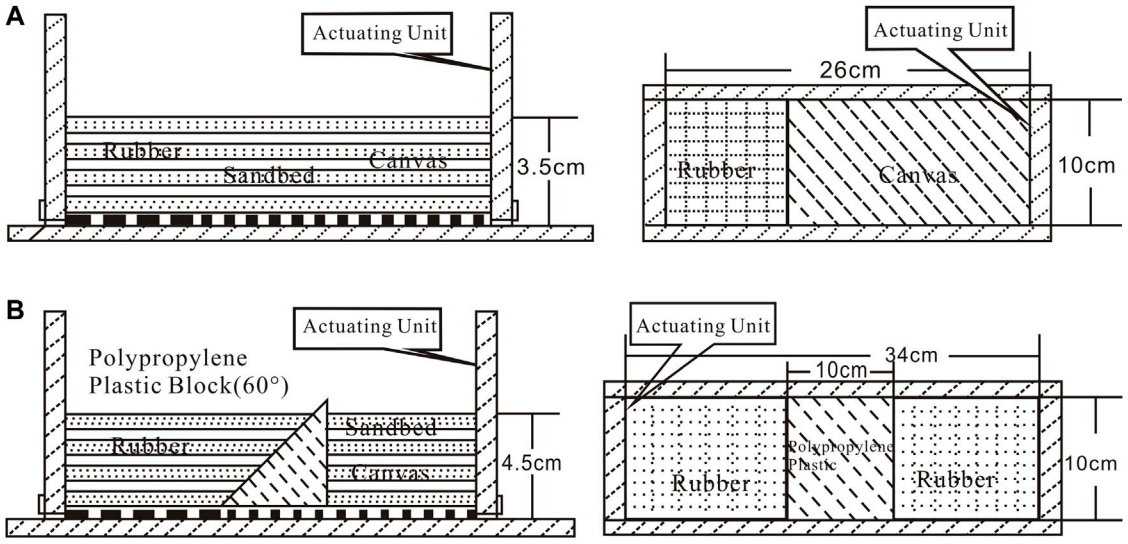

FIGURE 6
Basement conditions and experimental model of structural physical simulation experiment in the study area **(A)** Results of the tectonic physical simulation experiment for the T3–J3+K1 period **(B)** Results of the tectonic physical simulation experiment for the K2 period.

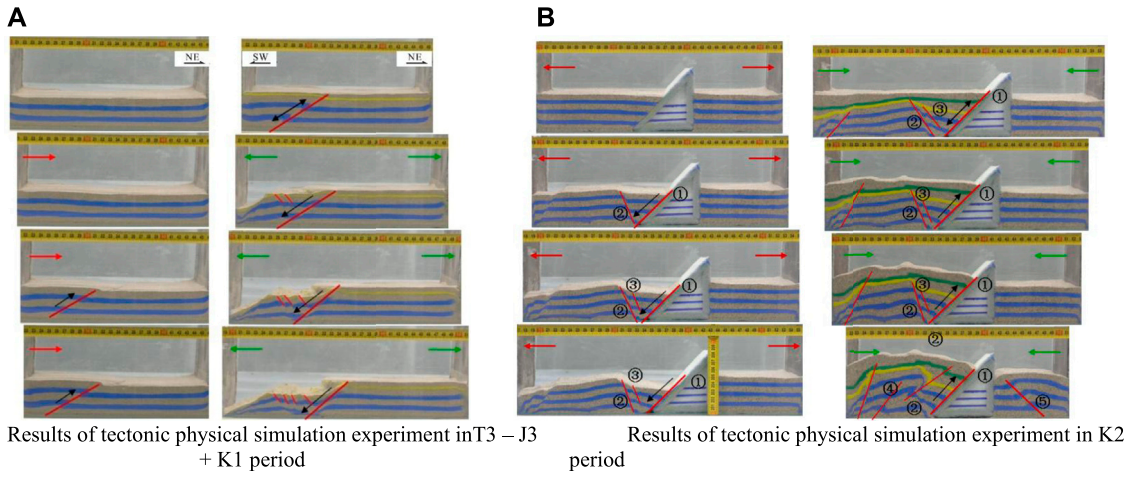

FIGURE 7
Results of the structural physics simulation experiment section in the study area. **(A)** Results of tectonic physical simulation experiment inT3-J3+K1 period; **(B)** Results of tectonic physical simulation experiment in K2 period.

transformed into the reverse fault with structure reversal (Figure 7B).

As extrusion displacement increased further, the inversion degree of the No. 1 Fault strengthened, and a series of new reverse faults were eventually generated. As a result, both the number and size of faults gradually increased. The lower plate of the No. 1 Fault generated new faults, but both their scale and number were small. The experiment ended after 92 min. Based on the comparison of multiple sets of simulation experiments, the early fracture system was found to be susceptible to reversal, which is consistent with the direction lines of the tensile and compressive stresses before and after reversal. If the direction of the tensile and extrusion stresses before and after inversion coincided with the section tendency, the early fracture system was vulnerable to reversal. Before and after the inversion, the directions of the tensile and extrusion stresses were the opposite of the section tendency, and a significant amount of friction resistance produced a new thrust fracture system. The experimental results revealed that in the study area, the stress-field transformation of the NW–SE trending initially exhibited tension and later displayed

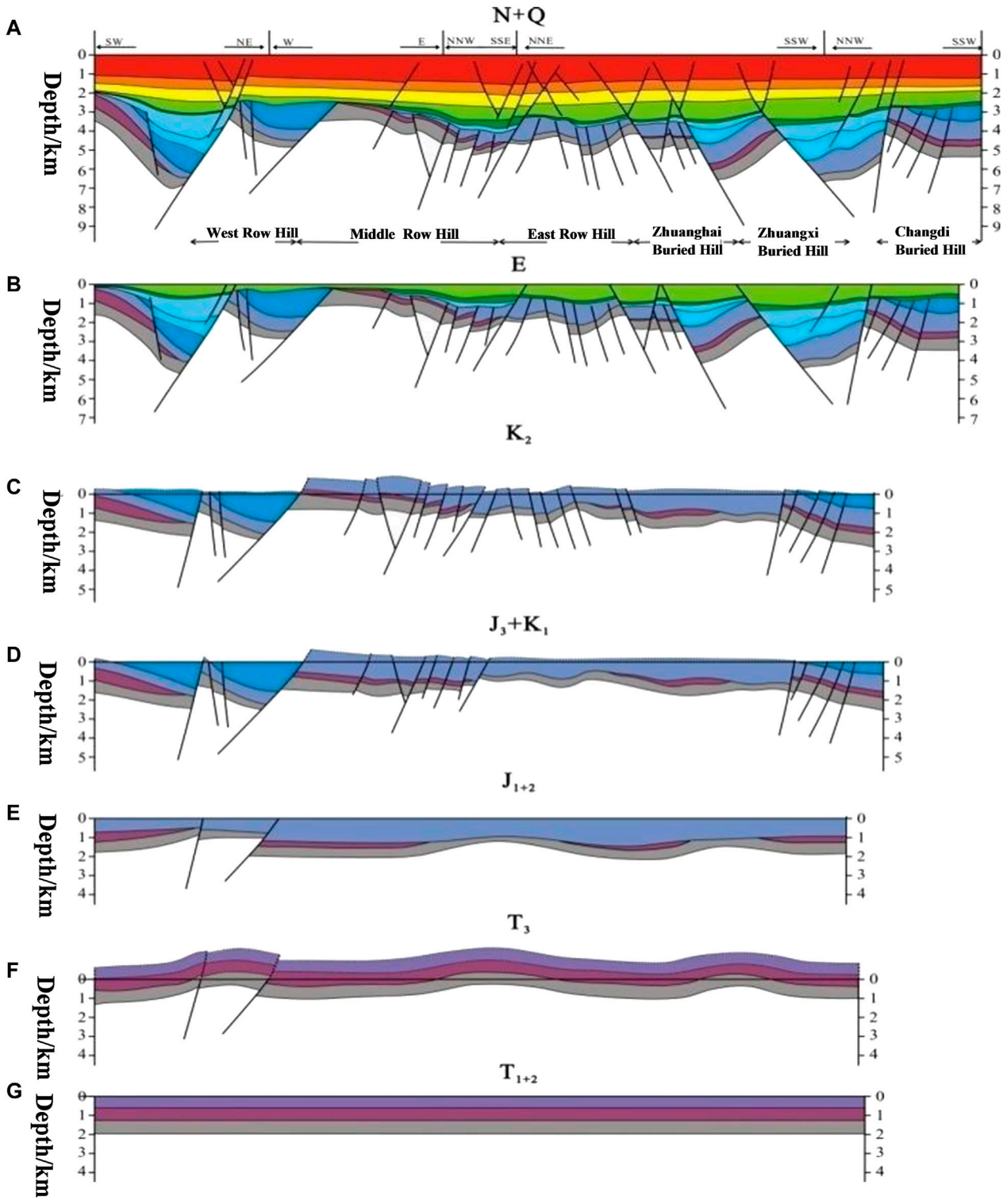

FIGURE 8
Typical structural balanced sections in the study area (refer to Figure 1 for details of section location). **(A)** Stratigraphic distribution in N+Q period; **(B)** Stratigraphic distribution in E period; **(C)** Stratigraphic distribution in K_2 period; **(D)** Stratigraphic distribution in J_3+K1 period; **(E)** Stratigraphic distribution in J_1+2 period; **(F)** Stratigraphic distribution in T_3 period; **(G)** Stratigraphic distribution in T_{1+2} period.

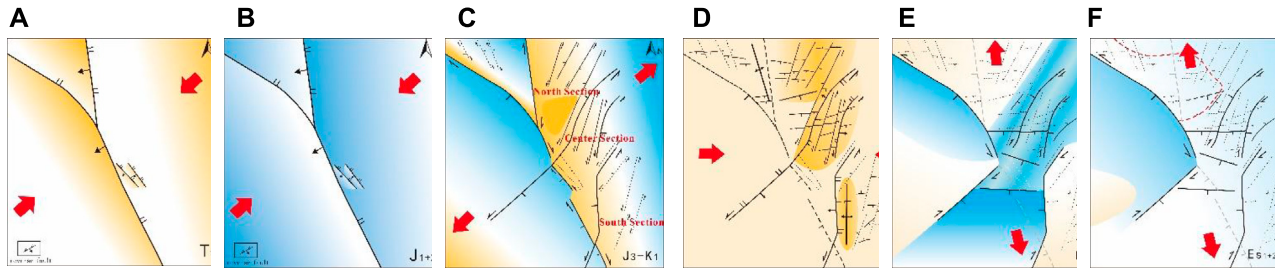

FIGURE 9
T3-E genetic model and structural framework changes in the study area. **(A)** genetic model and structural framework in T_3 period; **(B)** genetic model and structural framework in J_{1+2} period; **(C)** genetic model and structural framework in J_3+K1 period; **(D)** genetic model and structural framework in K_2 period; **(E)** genetic model and structural framework in Es_3 period; **(F)** genetic model and structural framework in Es_{1+2}-Ed period.

extrusion, which caused structural positive inversion in the earlier-formed normal faults. This result is consistent with the general positive inversion of the NE-trending faults in the K2 period of the Jiyang Depression.

5.2 Causes of the buried hill fault structure in the study area

Based on the interpretation of the discussed seismic profile and structural physical simulation experiment analysis, combined with the data sourced from previous studies, the formation of the buried hill fault structure in the Chengdao–Zhuanghai area is closely related to the significant transformation of the tectonic stress field in the study area and those adjacent to it since the late Triassic.

5.2.1 Overall uplift and erosion (Indosinian T_3)

The Yangtze plate converged and collided with the North China plate in the late stages of the Indo-Chinese movement (He, 2001), having a substantial impact on the tectonic pattern of the studied area (Qi, 2004). Controlled by the compressional collision between the North China plate and the Yangtze plate, the Jiyang depression is a regional stress field in the near-NNE of the compression system, which is in a state of uplift and erosion. Depletion of the Middle-Lower Triassic (Figures 8A,B) results in the development of a number of NW–NWW fold and thrust faults (Figure 9A). During this time, the Tanlu fracture belt did not affect the tectonic evolution of the Jiyang Depression. In particular, a series of NW-trending thrust faults were developed in the stress field of the Chengdao–Zhuanghai area, thereby forming an NW-trending thrust mountain-system tectonic pattern. Among these, the large-scale Chengbei–Wuhaozhuang fault zone exhibited significant activity that reached up to 120 m/Ma. Influenced by the regional compressive stress and NW-trending reverse fault activity, the overall uplift of the study area underwent erosion, and the peak of denudation was found in the upper plate of the NW-trending fault that was severely eroded near the fault side. The Upper Paleozoic and Lower Paleozoic were extensively or completely eroded, with prominent thin or bare-bottom phenomena. During this period, only the NW-trending faults developed in the Chengdao–Zhuanghai area, and the inner fault of the buried hill had not yet formed.

5.2.2 Overall filling deposits (Yanshanian J_{1+2})

During the early Yanshanian movement, the collision and extrusion between the Yangtze plate and the North China plate gradually weakened, and the influence of the western Pacific plate activity on the study area gradually increased. Eastern China began the transition between the Paleo-Asian and the Pacific tectonic stages (Zhou, 2006; Dong et al., 2007; Zhang et al., 2007).

A set of fluvial-lacustrine coal-bearing strata were deposited in the Jiyiang Depression over a protracted period of inland depressional subsidence, and they bear cap-type and NW-trending belt distribution characteristics. At this point, the Chengdao–Zhuanghai area had inherited the structural pattern of the late Triassic, and the overall depression deposition was still influenced by the NE–SW compressive stress field. However, the intensity of the activity was significantly lower in comparison with that of the Late Triassic, and the average activity rate was only −8 m/Ma. The area with a higher terrain exhibited less deposition, and that with a lower topography displayed a thicker deposition. The buried hills formed in the Late Triassic experienced the first burial (Figure 8C; 9B).

5.2.3 Fault segmentation (J_3-K_1, Mid-Yanshanian)

In the late Jurassic-early Cretaceous, the Yangtze plate and Siberia plate activities were replaced by the Pacific plate activity, which emerged as the primary control factor of the tectonic evolution in North China. This resulted in the formation of the Pacific tectonic domain. The NNW-trending subduction of the Pacific plate created a strong left-lateral strike-slip of the NNE-trending Tanlu Fault zone, which yielded a compressive–torsional tectonic stress field in eastern China. Simultaneously, the lithosphere in eastern China emerged strongly thinned, accompanied by mantle plume activity and asthenosphere uplift. Under the superposition of these two forces, eastern China entered a stage of large-scale rift development and thick strata deposition, accompanied by strong volcanic activity.

The research area was strongly affected by the left-lateral strike-slip of the Tanlu Fault zone. The NW-trending Chengbei

No. 5 Pile Fault exhibited a negative inversion that altered the original compressional thrust into an extensional fault. The strong fault activity and the average activity rates were approximately 30 m/Ma. The NW-trending buried hill system was initially formed when the bottom wall of the NW-trending fault was uplifted. The new NNE-trending left-lateral strike-slip fault occurred in the study area, whereas the right-lateral strike-slip activity occurred in the early NW-trending fault. The strike-slip activities of the NW-trending Chengbei–No. 5 Pile Fault and the NNE-trending Chengbei 30 North–Chengdong Fault in the late Cretaceous generated regional conjugate pressurization between the two faults. In addition, numerous NNE-trending compressive–torsional strike-slip faults were formed within the Middle Row Hill and East Row Hill owing to the influence of the compressive–torsional tectonic stress-field throughout eastern China. A small amount of strike-slip extensional faults was formed under the strike-slip activities in the west row of the fault between the NW-trending Chengbei Fault and the NNW-trending Chengbei 20 Fault. As of this moment, a series of strike-slip faults similar to those in the Tanlu Fault zone have been determined in the study area, cutting the NW-trending buried hill system. This occurrence complicated the NW-trending mountain system and segmented it into the north, middle, and south sections (Figure 8D; 9C).

5.2.4 Extrusion uplift differentiation (late Yanshanian K_2)

In the late Cretaceous, the Pacific Plate transformed into a low-velocity northward movement, resulting in the retreat of trenches and plates. The trench retreat vector shifted southward, and the east of the North China Craton appeared to be stretched along the near-SN direction. During this stage, the near-EW extrusion formed the near-SN thrust structure, and the entire area was uplifted and eroded (Zhang and Dong, 2008). Partially formed in the late Jurassic–early Cretaceous NNE strike-slip faults (distributed in Middle Row Hill, East Row Hill, and Zhuanghai Buried Hill) by compressive and torsional activities, a series of new near-EW-trending secondary normal faults were also formed. Among them, the fault activity of Chengbei 8 was strong and lowered the southern part of the Middle Row Hill in the high region of the late Jurassic–early Cretaceous with relatively moderate denudation. In their entirety, the NNE and near-EW faults were further complicated. The near-EW compressional structure enhanced the NNE-trending mountains (Figure 8E, Figure 9D).

5.2.5 Mid-subduction differentiation (early himalayan period E)

The sedimentary period of the Kongdian Formation-Sha 4 member represents the transition period between the Yanshan movement and the Himalayan movement. At this stage, the subduction direction of the Pacific plate persisted in the NNW direction, and the Tanlu Fault zone inherited the Yanshan movement mode, which corresponded to the left-lateral strike-slip (Li et al., 2019). The NW-trending Chengbei Fault inherited this activity and maintained its strength, whereas the NW-trending Chengbei 20 Fault and No. 5 Pile Fault started to diminish. The NNE-trending Chengbei 30 South Fault, the Chengdong Fault, and the Changdi Fault started to resurface. In the vicinity of the EW-trending Chengbei 304 South Fault, the Zhuanghai 104 South Fault, and the Zhuangnan fault formed and started to move, thereby regulating certain depositions. Only a small portion of the Zhuanghai and Zhuangxi Buried Hills started to receive deposition during this time, and other buried hills were still undergoing exposure and erosion (Figure 8F, Figures 9E–F).

A regional tectonic movement known as the Jiyang event, which was an essential tectonic movement in the development of the Jiyang Depression (Zhu & Xu, 2019) occurred in the Sha3 layer. During the Cenozoic, the Pacific plate and Indian Ocean plate surrounding Eurasia underwent major kinematic adjustments. The movement direction of the Pacific plate varied from NNW to NWW, which was positively subducted beneath Eurasia. The collision of the Indian subcontinent with the Eurasian plate was eventually completed at the end of the Middle-Eocene. As a result, the Tanlu Fault rotated from left to right, resulting in the formation in the area of an NW-trending extensional stress field. The NE- and EW-trending faults in the study area became strongly active and developed as the Cenozoic basin-controlling faults in the study area (Feng J et al., 2017; Du et al., 2020). Owing to the coupling of the strong activities of the Chengbei 304 South Fault, Zhuanghai 104 South Fault, and Zhuangnan Fault, the Zhuanghai and Zhuangxi Buried Hills were completely covered. The eastern mountain is still topographically controlled by terrain, some areas are subject to sedimentation, and other areas are still exposed to the water surface and being eroded (Figure 9E).

In the Sha 2 and Sha 1 layers, the overall stress field characteristics of the study area were similar to those of the Sha 3 Formation. However, the relative strengths of the right-handed shear stress and horizontal tensile stress started to change, which weakened the tensile stress and gradually increased the shear stress. Even if the entire fault system exhibited inheritance, the active strength started to weaken. Although the activity rates of the NNE-trending and near EW-trending primary faults in the study area were significantly lower than those of Sha 3, numerous secondary NNE-trending and near EW-trending faults continued to exist. Among these faults, the transformation of NNE-trending faults onto the structural pattern was more evident. During this period, East Row Hill and Changdi Buried Hill were completely interred, and Middle Row Hill was partially buried. During the sedimentary period of the Dongying Formation, the structural pattern inherited the sedimentary period of the Sha 2 and Sha 1 layers, with a dominant NEE-oriented fault activity. The number of NNE-trending right-lateral strike-slip faults (or extensional strike-slip faults) and derived NEE-trending secondary faults increased drastically. In the local regions, the primary faults started being discontinuous, and the strike-slip effect became more pronounced (Figure 9F).

5.2.6 Overall stable subsidence (late himalayan N + Q)

The entire Chengdao–Zhuanghai area entered the subsidence stage in the Neogene, during which the fault activity in all directions decreased significantly and the primary faults in all directions became intermittent. Consequently, a series of *en-échelon* secondary faults developed along the direction of the primary fault, and the influence of strike-slip movement gradually

increased from west to east. Compared with the previous period, the fault activity rate was considerably reduced. The buried hills in the study area remained deeply buried (Figure 8G). The section location is presented in Figure 1.

In conclusion, the thrusting activity of the NW-trending faults in the late Triassic and the tectonic inversion of the late Jurassic to early Cretaceous shaped the NW-trending Buried Hill system in the research area. The left-lateral strike-slip fault of the Tanlu Fault zone yielded the NNE-trending synclinal strike-slip fault, which divided the NW-trending mountain system and segmented it into three sections: north, middle, and south. The core of the buried hill is further complicated by the EW-trending extensional faults that developed in the late Cretaceous, and the NNE- and NW-trending strike-slip faults that formed in the late Jurassic to early Cretaceous. Until the Palaeogene, the Tanlu Fault fluctuated from left-handed activity to right-handed activity, and near-EW-trending normal faults were observed in the study area, which transformed the middle part of the mountain system into a buried hill with a near-EW-trending distribution. After the sedimentary period of the Dongying Formation, the overall subsidence received the deposition that formed the current structural pattern of the buried hill.

6 Relationship between faults and oil distribution in the buried hills

Chengbei, Shanan, Bozhong, Huanghekou, Gubei, and other oil-generating depressions are distributed throughout the buried hills in the Chengdao-Zhuanghai area, with adequate oil and gas supply and suitable oil source conditions. The Chengbei Fault, the Changdi Fault, and the Chengbei 20 Fault are the three main NW trending faults. In particular, the Chengbei and Changdi faults have been active for a long time and can be used as channels for oil and gas migration. The stratum dip traverses in the opposite direction from the fault dip. As the oil and gas migration cannot easily fill the buried hill, the oil and gas reservoir in the buried hill is small, whereas the upper Guantao Formation and Dongying Formation are large. The Chengbei Fault, along which the oil and gas are partially filled, forms the west boundary fault of the Chengdao Buried Hill. Similarly, the Changdi Fault forms the west boundary fault of the Changdi Buried Hill, with oil and gas migrating upward along the Changdi Fault along the Gubei Sag in the west, and with some of this migration occurring southward along the structural beam of the Changdi Low Uplift in the northeast. Furthermore, the Changdi Fault regulates the oil-bearing boundary of the Changdi Buried Hill. Owing to the shallow burial in this area, the buried oil and gas pool is small. Specifically, the Chengbei 20 Fault forms the west boundary of the Zhongpai Mountain in the Chengdao Buried Hill. The oil source in the Chengbei Zhongpai Mountain originates in the northern Shanan Depression and moves south along the structural beam. Therefore, the Chengbei 20 Fault controls the oil-bearing property of the Zhongpai Mountain, and the oil and gas are primarily distributed along the structurally high regions of the Zhongpai Mountain.

Overall, the presence of multiple NE-trending faults has created three main structural beams that control the oil and gas migration channels, forming the distribution characteristics of oil and gas enrichment in the structural beams.

The NEE-trending faults can be segmented into small faults and boundary large faults, where small faults complicate the distribution of oil and gas. These faults exhibit various sealing properties depending on the fault-filling cementation and dissolution. In principle, the degree of sealing controls both the height and distribution of oil and gas. Oil- and gas-bearing properties are identified by the well-sealed fault's rising wall. The lower collapsing wall is devoid of the oil and gas injection that created the oil difference in the buried hill fault block. Primarily, the main faults include the Chengbei 304 South Fault, the Zhuanghai 104 South Fault, and the Zhuangnan Fault, all of which are Nandiao reverse faults. The Chengbei 304 and Zhuanghai 104 South Faults contained the formation of the buried hill reservoir and hindered the oil and gas migration from several similar channels in the northeast. This generated the most abundant distribution of oil and gas north of the Chengbei 304 South Fault, followed by the Zhuanghai 104 South Fault. The Zhuangnan Fault blocked the oil and gas that formed in the Chengbei Sag and Zhuangxi Sag and controlled the south boundary of Zhuangxi Buried Hill.

7 Discussion and conclusion

Fault structure is the most important controlling factor for buried hill reservoirs in the Chengdao–Zhuanghai area. The inner fault of the NW-trending buried hill in this area is similar to the strike-slip extensional fault formed by the right-lateral strike-slip movement of the NW-trending Chengbei Fault in the late Jurassic-early Cretaceous eras. More specifically, the NNE-trending fault is a left-handed compression–torsion fault that developed under the left-handed strike-slip activity and the regional compression stress field of the Tanlu Fault zone. Furthermore, the near-EW fault is closely associated with the near-SN extension stress field in the late Cretaceous.

The current research provided the following insights.

1. NW-trending faults govern the formation of "mountains": faults have undergone the stable craton, compression thrust, denudation and leveling, and structural inversion stages. The NW-trending fault was formed by the compressional thrust in the late Triassic. After that, it experienced a tectonic inversion process that ranged from a thrust to a normal fault in the Mesozoic. In the Cenozoic, the Chengbei Fault was inherited and developed, whereas the Chengbei 20 Fault disappeared.
2. The cutting of an NNE (NE)-trending fault into an NW trending "mountain system" segmented the mountain system in the study area into three sections: north, middle, and south. The NNE (NE) trending fault was formed in the J3-K1 period, which experienced a transformation from J3 to K1 left-handed to K2 compressional torsional to E right-handed tensional torsion. The section formed a flower-like and multistage Y-shaped combination due to its relative steepness. Owing to the transformation from the NW to the Chengbei No. 5 Pile Fault, the Chengbei 30 North and Chengbei 30 South Fault groups formed horsts, and the

Chengdong and Changdi faults generated grabens. The strata on both sides of the Changdi Fault bent violently and were compressed in the Late Cretaceous, creating forced folds.

3. The EW-trending fault cut the NNE-trending zone to form the Dongpaishan, Zhuanghai, and Zhuangxi Buried Hill "mountains", wherein most EW-trending faults were Cenozoic active faults. The peak activity occurred in Es3, which is a typical shovel-type normal fault. The EW-trending fault separated the Dongpaishan, Zhuanghai, and Zhuangxi Buried Hills from the middle section of the buried hills in the study area.
4. The superposition effect of the multiple faults resulted in the complexity and diversity of the "mountain" structures.
5. The oil and gas reservoirs currently discovered were primarily concentrated in the Lower Paleozoic. The Ordovician served as the primary reservoir, and the pores, caves, and fractures that developed along the top surface of the Ordovician carbonate rock created the primary reservoir spaces (Kong and Lin, 2000; Li et al., 2004; Li et al., 2000; Feng, et al., 2019; Du, et al., 2022).

In total, five types of traps were developed in the lower Paleozoic, including fault block traps, fault nose traps, residual hill traps, unconformity traps, and compression twist-fold traps, with fault block traps having the greatest density and the most extensive distribution.

6. The formation of buried hill reservoirs was determined based on the effective hydrocarbon source rocks, reservoirs, migration pathways, traps, preservation conditions, and their spatiotemporal configuration in the Chengdao–Zhuanghai area (Yang et al., 2001; Qiu et al., 2010). In the study area, the buried hill reservoirs were the most abundant in the NW and NNE fault conjugate locations (Feng et al., 2021). The oil sources for Zhongpaishan, Dongpaishan, and other buried hill reservoirs were found in the east and north Shanan Sags as well as Bozhong Sags, which exhibited the characteristics of migration and accumulation along the parallel fault in the far source.
7. The oil source of the northwest Chengbei and Changdi faults primarily originated on the downthrow side of the faults, and the oil and gas migration occurred upward along the faults. Therefore, the favorable reservoir inside the buried hill matched the direction of oil and gas exploration. In the Chengbei 20 fault, oil and gas mainly originated from the unconformity surface of the buried hill to the north. As a result, the fault block parallel to the direction of the oil and gas migration represents the path of future exploration and development. The NE-trending fault controlled the shape and distribution of the top surface of the buried hill, thereby forming three structural beams. Numerous fault blocks were created as a result of the NE-trending fault and the NNE-trending fault cutting each other. Overall, the buried hill fault block along the lower portion of the structural beam indicated the direction of oil and gas exploration.

In conclusion, the systematic understanding of the fault structure characteristics and genetic mechanism, which confirms the impact of multiple sets of unconformity and various faults in the area on the migration and accumulation of oil and gas in buried hills, allows for further exploration of the differential oil and gas migration and accumulation characteristics in different buried hills. As such, this finding highlights the favorable direction of exploration. Furthermore, fault sealing under the influence of multiple parameters can be quantitatively evaluated to provide a systematic, comprehensive fault-sealing prediction method with great scientific value.

Data availability statement

The original contributions presented in the study are included in the article/Supplementary Material, further inquiries can be directed to the corresponding author.

Author contributions

ZW, KZ, and QW contributed to conception and design of the study. HZ organized the database and experiment. SY, YL performedthe statistical analysis. ZW, KZ, and QW wrote the first draft of the manuscript. SY and YL wrote sections of the manuscript. All authors contributed to manuscript revision, read, and approved the submitted version.

Funding

The work throughout the conception, design, and publication of this Research Topic was supported by the National Natural Science Foundation of China (42072234).

Acknowledgments

We would like to thank all the reviewers and authors for their contributions to this Research Topic. We also thank the entire team at Frontiers in Earth Science for their dedicated effort in guiding the revision and detailed editing of the papers on the Research Topic.

Conflict of interest

ZW, QW, HZ, SY, and YL were employed by Haiyang Oil Production Plant, Shengli Oilfield Company, Sinopec

The remaining author declares that the research was conducted in the absence of any commercial or financial relationships that could be construed as a potential conflict of interest.

Publisher's note

References

Chen, G., and Zhang, S. (2002). Discussion on the exploration of low buried hills between Chengdao and Zhuangxi areas. *Pet. Exp. Geol.* 24 (4), 306–310. doi:10.3969/j.issn.1001-6112.2002.04.004

Dai, J., and Meng, Z. (2000). Finite strain study on paleozoic structures in Chengdao region. *J. Geomechanics* 6 (1), 77–83. doi:10.3969/j.issn.1006-6616.2000.01.010

Dong, S., Zhang, Y., Long, C., Yang, Z., Ji, Q., Wang, T., et al. (2007). Jurassic tectonic revolution in China and new interpretation of the Yanshan Movement. *Acta Geol. Sin.* 81 (11), 1449–1460. doi:10.3321/j.issn:1000-9515.2008.02.012

Du, H., Feng, J., Xu, S., Shang, S., and Li, C. (2022). Quantitative characterization of volcanic expansion fractures based on thermodynamic coupling analysis. *Geoenergy Sci. Eng.* 221, 211387. doi:10.1016/j.geoen.2022.211387

Du, H., Xu, S., Feng, J., Ren, Q., Wang, Z., and Xu, K. (2020). Digital outcrop representation for karst fracture-cave reservoir. *J. China Univ. Petroleum(Edition Nat. Sci.* 44 (5), 1–9. doi:10.3969/j.issn.1673-5005.2020.05.001

Feng, J., Qu, J., Wan, H., and Ren, Q. (2021). Quantitative prediction of multiperiod fracture distributions in the cambrian-ordovician buried hill within the futai oilfield, Jiyang depression, east China. *J. Struct. Geol.* 148, 104359. doi:10.1016/J.JSG.2021.104359

Feng, J., Sun, Z., Wang, Y., and She, J. (2019). Study on stress sensitivity of ordovician fractures in hetianhe gas field, tarim basin. *Geol. J. China Univ.* 25 (2), 276–286. doi:10.16108/j.issn1006-7493.2018059

Feng, J., Wang, Z., and Shang, L. (2017). Genetic mechanisms of superimposed fault systems in block 3 of nanpu SagBohai Bay Basin. *OIL&GAS Geol.* 38 (6), 1032–1042. doi:10.11743/ogg20170603

Guo, F., Hou, S., Liu, R., Xia, B., Yuan, Y., and Wan, Z. (2012). Balanced cross-section for restoration of structural evolution in a foreland thrust belt: Taking the northwestern margin of junggar basin for example. *Mar. Geol. Front.* 28 (12), 46–51. doi:10.16028/j.1009-2722.2012.12.005

He, B. (2001). On dynamics of the Bohai Bay complex faulted basin. *Pet. Geol. Exp.* 23 (1), 27–31. doi:10.3969/j.issn.1001-6112.2001.01.005

Hou, F., Li, S., Wang, J., Yu, J., Lv, H., and Xu, S. (2005). Buried hill fault in Zhuanghai area of Jiyang depression. *Mar. Geol. Quater. Geol.* 25 (3), 69–74. doi:10.16562/j.cnki.0256-1492.2005.03.010

Hu, Q., Dong, D., Yang, J., Gao, L., Kong, X., Yang, G., et al. (2020). Geostructural analysis and physical simulation for the 4th block of the central Junggar Basin. *Sci. Technol. Eng.* 20 (10), 3898–3907. doi:10.3969/j.issn.1671-1815.2020.10.015

Hu, W. (1997). The types of forward and inversion structures and their research methods. *Daqing Pet. Geol. Dev.* 16 (2), 6–9. doi:10.19597/j.issn.1000-3754.1997.02.002

Jing, A. (2020). Characteristics and control of faults on reservoir of Lower Paleozoic buried hill in Chengdao area, Jiyang depression. *Sci. Technol. Engin.* 20 (15), 6011–6017. doi:10.3969/j.issn.1671-1815.2020.15.018

Jiu, K., Ding, W., Huang, W., You, S., Zhang, Y., and Zeng, W. (2013). Simulation of paleotectonic stress fields within Paleogene shale reservoirs and prediction of favorable zones for fracture development within the Zhanhua Depression, Bohai Bay Basin, east China. *J. Pet. Sci. Eng.* 110, 119–131. doi:10.1016/j.petrol.2013.09.002

Kong, F., and Lin, H. (2000). Characteristics of buried hill reservoirs in Chengdao area. *J. Chengdu Inst. Technol.* 27 (2), 116–122. doi:10.3969/j.issn.1671-9727.2000.02.002

Li, L., and Dai, J. (2000). Numerical simulation of tectonic stress field and fracture distribution of Mesozoic and Paleozoic erathem in Chengdao area. *J. UnivPet. China (Ed. Nat. Sci.* 24 (1), 6–9. doi:10.3321/j.issn:1000-5870.2000.01.002

Li, P., Zhang, S., Wang, Y., and Ma, L. (2004). Study on the Genesis and reservoir formation of diversified buried hills in fault basin taking Jiyang Depression as an example. *J. Pet.* 25 (3), 29–31. doi:10.3321/j.issn:0253-2697.2004.03.005

Li, S., Xianzhi, C., Guangzeng, W., Zhaoxia, J., Wang, P., Gang, W., et al. (2019). Meso-Cenozoic tectonic evolution and plate reconstruction of the Pacific Plate. *J. Geomech.* 25 (5), 642–677. doi:10.12090/j.issn.1006-6616.2019.25.05.060

Li, W., Wu, Z., and Zhao, W. (2010). Yanshanian tectonic characteristics and basin transformation in Bohai Bay basin area. *Prog. Geophys.* 25 (6), 2068–2077. doi:10.3969/j.issn.1004-2903.2010.06.024

Li, Y. (2008). Hydrocarbon enrichment regularity and exploration of buried hill in Bohai Bay Basin. *J. Mar. Geol. Dyn.* 24 (3), 1–7. doi:10.3969/j.issn.1009-2722.2008.03.001

Li, Z., Dong, S., and Qu, H. (2014). Sedimentary evidences of jurassic orogenic process and key time limit on the northern margin of North China craton. *J. J. Jilin University: Earth Sci. Ed.* 5, 1553–1574. doi:10.13278/j.cnki.jjuese.201405113

Liu, Y., and Wu, Z. (2019). Cenozoic fault system and tectonic framework of Chengbei Sag and its adjacent areas, Bohai Bay Basin. *Geotect. Metallogenia* 43 (6), 1133–1143. doi:10.11817/j.issn.1672-7207.2022.03.029

Ma, L., Wang, Y., Jing, A., Yang, G., Wu, Y., and Zhao, M. (2018). Palaeogene structural style and its reservoir control in the beach area of Jiyang Depression. *Oil Gas. Geol. Recov.* 25 (1), 1–5. doi:10.13673/j.cnki.cn37-1359/te.2018.01.001

Mao, L., Tian, J., Wang, L., Zhang, C., Zhang, W., Tian, R., et al. (2019). Initiation and origin of dextral deformation at mid-eocene in the Western Bohai Bay Basin, east China. *J. Asian Earth Sci.* 185, 104031. doi:10.1016/j.jseaes.2019.104031

Qi, J. (2004). Two tectonic systems in the Cenozoic Bohai Bay basin and their genetic interpretation. *Geol. China* 31 (1), 15–22. doi:10.3969/j.issn.1000-3657.2004.01.002

Qiu, Y., Wand, Y., and Liu, W. (2010). Study on internal structure and migration in fault zones. *Pet. Geol. Recov. Eff.* 17 (4), 1–3. doi:10.3969/j.issn.1009-9603.2010.04.001

Shi, X. (2021). Study on characteristics and sealing of buried hill faults in Chengdao area, Jiyang Depression. *Complex Hydrocarb. Reserv.* 14 (3), 1–7. doi:10.16181/j.cnki.fzyqc.2021.03.001

Wang, Y., Wang, Y., and Zhao, X. (2004). The influence of tectonic evolution of Jiyang Depression on the formation of fault block buried hill and hydrocarbon reservoir. *Mineral. Rock* 24 (2), 73–77. doi:10.19719/j.cnki.1001-6872.2004.02.015

Wei, Z., Zhang, L., Shuai, Q., Yi, H., Qian, X., Lei, Z., et al. (2018). Application of balanced cross section technique to the study of tectonic evolution of Western Taiwan Strait Basin. *Mar. Geol. Quater. Geol.* 38 (5), 193–201. doi:10.16562/j.cnki.0256-1492.2018.05.019

Xie, Z. K. (2011). Sequence boundaries and regularities in the oil-gas distribution of the low swelling slope belt in the continental rift basin. *Min. Sci. Technol. (China)* 21 (3), 419–425. doi:10.1016/j.mstc,2011.05.011

Xie, Z., Wang, Z., Ming, Y., Wang, M., Zhang, Z., Yang, B., et al. (2021). Cenozoic fault system in the southern East Chengdao low rise of Bohai Sea area and its control on oil and gas distribution. *Earth Sci. Front.* 28 (5), 413–420. doi:10.13745/j.esf.sf.2021.1.62

Xin, Y., Liu, H., Ma, L., and Tian, W. (2021). The controlling factors of oil and gas differential accumulation in Chengdao buried hill. *Geol. Rev.* 67 (S1), 235–236. doi:10.16509/j.georeview.2019.s1.087

Yang, F., Zhou, Z., and Liao, Y. (2001). Hydrocarbon migration and accumulation system analysis for Chengdao complicated oilfield. *J. Tongji Univ. Nat. Sci. Ed.* 29 (07), 838–844. doi:10.3321/j.issn:0253-374X.2001.07.016

Yang, M. (2008). Comparative analysis of buried hill diversity and reservoir forming elements in Bohai Bay Basin. *Pet. Nat. Gas. Geol.* 29 (5), 621–631. doi:10.3321/j.issn:0253-9985.2008.05.011

Zhang, G., Huang, J., Lu, X., Wang, Z., and Shi, Z. (2022). Ordovician limestone boundary structural factor analysis in Qipanjing Minefield. *Zhuozishan Coalf. based Tect. Phys. Simul. Exp.* 34 (2), 10–18. doi:10.3969/j.issn.1674-1803.2022.02.03

Zhang, M., Fu, J., and Yin, X. (2006). Characteristics of strike slip and compression structures in Zhuanghai area. *Oil Gas. Geol. Recov. Fact.* 13 (02), 5–8. doi:10.3969/j.issn.1009-9603.2006.02.002

Zhang, X., Wu, Z., Zhou, X., Niu, C., Li, W., Ren, J., et al. (2017). Cenozoic tectonic characteristics and evolution of the southern Bohai sea. *Geotect. Metallogenia* 41 (1), 50–60. doi:10.16539/j.ddgzyckx.2017.01.004

Zhang, X. (2006). Structural style of pre-Tertiary buried hill in Zhuanghai area of Jiyang depression. *Oil Gas. Geol. Recov.* 13 (4), 12–14. doi:10.3969/j.issn.1009-9603.2006.04.004

Zhang, Y., and Dong, S. (2008). Mesozoic tectonic evolution history of the Tan—Lu fault zone, China: Advances and new understanding. *Geol. Bull. China* 27 (9), 1371–1390. doi:10.3969/j.issn.1671-2552.2008.09.002

Zhang, Y., Dong, S., Zhao, Y., and Zhang, T. (2007). Jurassic tectonics of North China: A synthetic view. *Acta Geol. Sin.* 81 (11), 1462–1480. doi:10.3321/j.issn:1000-9515.2008.02.010

Zhou, X. (2006). Major transformation and thinning of subcontinental lithosphere beneath eastern China in the cenozoic–mesozoic: Review and prospect. *Earth Sci. Front.* 2 (13), 50–64. doi:10.3321/j.issn:1005-2321.2006.02.004

Zhu, R., and Xu, Y. (2019). The subduction of the west Pacific plate and the destruction of the North China Craton. *Sci. China Earth Sci.* 62, 1340–1350. doi:10.1007/s11430-018-9356-y